Propensity for distinguishing two free electrons with equal energies in electron-impact ionization of helium

Xueguang Ren,[1,2,*] Arne Senftleben,[2,3] Thomas Pflüger,[2] Klaus Bartschat,[4] Oleg Zatsarinny,[4] Jamal Berakdar,[5] James Colgan,[6] Michael S. Pindzola,[7] Igor Bray,[8] Dmitry V. Fursa,[8] and Alexander Dorn[2]

[1]*Physikalisch-Technische Bundesanstalt, D-38116 Braunschweig, Germany*

[2]*Max-Planck-Institut für Kernphysik, D-69117 Heidelberg, Germany*

[3]*Universität Kassel, Institut für Physik, Heinrich-Plett-Strasse 40, D-34132 Kassel, Germany*

[4]*Department of Physics and Astronomy, Drake University, Des Moines, Iowa 50311, USA*

[5]*Institut für Physik, Martin-Luther Universität Halle-Wittenberg, D-06099 Halle/Saale, Germany*

[6]*Theoretical Division, Los Alamos National Laboratory, Los Alamos, New Mexico 87545, USA*

[7]*Department of Physics, Auburn University, Auburn, Alabama 36849, USA*

[8]*Curtin Institute for Computation and Department of Physics and Astronomy, Curtin University, GPO Box U1987, Perth WA6845, Australia*

(Received 27 August 2015; published 16 November 2015)

We report a combined experimental and theoretical study on the electron-impact ionization of helium at $E_0 = 70.6$ eV and equal energy sharing of the two outgoing electrons ($E_1 = E_2 = 23$ eV), where a double-peak or dip structure in the binary region of the triple differential cross section is observed. The experimental cross sections are compared with results from convergent close-coupling (CCC), *B*-spline *R*-matrix-with-pseudostates (BSR), and time-dependent close-coupling (TDCC) calculations, as well as predictions from the dynamic screening three-Coulomb (DS3C) theory. Excellent agreement is obtained between experiment and the nonperturbative CCC, BSR, and TDCC theories, and good agreement is also found for the DS3C model. The data are further analyzed regarding contributions in particular coupling schemes for the spins of either the two outgoing electrons or one of the outgoing electrons and the 1*s* electron remaining in the residual ion. While both coupling schemes can be used to explain the observed double-peak structure in the cross section, the second one allows for the isolation of the exchange contribution between the incident projectile and the target. For different observation angles of the two outgoing electrons, we interpret the results as a propensity for distinguishing these two electrons—one being more likely the incident projectile and the other one being more likely ejected from the target.

DOI: 10.1103/PhysRevA.92.052707 PACS number(s): 34.80.Dp

I. INTRODUCTION

The interaction of electrons with matter is of fundamental importance in a wide variety of scientific and practical applications for the understanding of the collision dynamics and the structures of matter in the fields of physics, chemistry, biology, and surface science [1,2].

Two outgoing electrons usually emerge in electron-impact ionization of matter. One of these electrons is generally the scattered projectile while the other one is the secondary electron originating from the ejection of a target bound electron in a so-called $(e,2e)$ reaction. A comprehensive way of characterizing the dynamics of the $(e,2e)$ ionization process is to detect the two outgoing electrons in coincidence. This is a kinematically complete experiment, in which the linear momentum vectors of all final-state particles are determined. Such experiments serve as a powerful tool to understand the quantum few-body problem [3,4]. The quantity measured in such experiments is the triple-differential cross section (TDCS), i.e., a cross section that is differential in the solid angles of both electrons and the energy of one of them. The energy of the other electron is given by energy conservation.

Electron-impact ionization of atoms and molecules has been extensively studied by theory and experiment due to its basic role as the fundamental few-body system (see, for example, [5–29]). Today, the measured TDCS, even in three-dimensional (3D) representations, can be well reproduced by the most sophisticated nonperturbative theories, particularly for simple (quasi-)one- and (quasi-)two-electron targets such as H, He, or the light alkali-metal and alkaline-earth-metal elements. Sophisticated perturbative models may also give detailed insight into the most important interactions and mechanisms, since they can generally be modified more easily compared to approaches that concentrate on solving the underlying quantum mechanical equations to the highest degree of numerical accuracy currently possible.

Recently, studies on the ionization of helium by electron impact ($E_0 = 70.6$ eV) reported excellent agreement between experiment and theoretical predictions from the convergent close-coupling (CCC) and time-dependent close-coupling (TDCC) methods [20]. Moreover, an additional node structure was observed in the binary region of the TDCS at $\theta_1 = -30^\circ$ and equal energy sharing ($E_1 = E_2 = 23$ eV); see the kinematics in Fig. 1. Such a feature is unexpected for ionization of a He(1*s*) electron [3,4].

According to the principles of quantum mechanics, the two free electrons resulting from the electron-impact ionization process are experimentally indistinguishable. Nevertheless, for highly asymmetric *energy* sharing, one often refers to the faster of the two outgoing electrons as the "scattered projectile," while the slower one is considered as the "ejected electron." This classification is due to a propensity based on a classical picture, but it would obviously not be applicable in the

*ren@mpi-hd.mpg.de

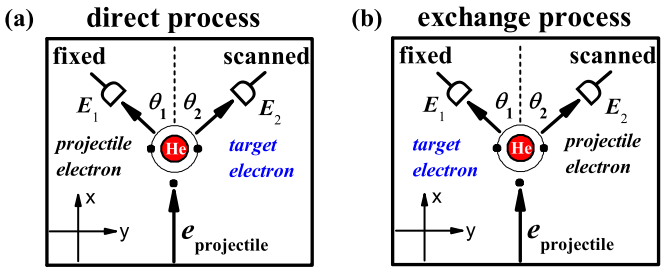

FIG. 1. (Color online) Sketch of the $(e,2e)$ reaction for the direct scattering process (a) and the exchange process (b).

equal-energy sharing case. The question, however, remains, whether such a propensity rule can be established based on different observation *angles* of the two electrons.

In order to investigate whether such a propensity might, indeed, contribute to the observed nodal structure in the TDCS for helium [20], we continued our study on electron-impact ionization of helium with the kinematic conditions mentioned above, i.e., $E_0 = 70.6$ eV; $E_1 = E_2 = 23$ eV. The TDCS was measured at different sets of scattering angles in the range $-50^\circ \leqslant \theta_1 \leqslant -35^\circ$, which corresponds to the momentum transfer in the range 1.75 a.u. $\geqslant q \geqslant$ 1.42 a.u.. The present experiments are compared with a number of theoretical predictions. In addition to the CCC and TDCC theories mentioned above, we employed the *B*-spline *R*-matrix-with-pseudostates (BSR) [30] approach, as well as the dynamic screening three-Coulomb (DS3C) [8] method.

Based on a general interpretation of the $(e,2e)$ experiment with one detector at a fixed angle and the other detector scanning the entire angular range, three distinct pathways can contribute to the TDCS [3,31]. They are (i) the direct scattering process, for which the scattered projectile is fixed to one emission direction (labeled "θ_1," even though we will see that this notation may not be appropriate) while one scans the angle of the ejected electron (labeled "θ_2"), as shown schematically in Fig. 1(a); (ii) the exchange process, in which the roles of the two outgoing electrons are interchanged as shown in Fig. 1(b); and (iii) the capture process, in which both target electrons are promoted into the continuum while the projectile electron is captured into a bound state of the residual ion. In the present work, we neglect the capture channel.

II. EXPERIMENTAL METHOD

The experiment was performed with a reaction microscope, purpose-built for electron collision [32]. Details of the experimental setup were described elsewhere [20]. Briefly, a pulsed electron beam ($\Delta T \approx 1.5$ ns), produced by a standard thermo-cathode gun, intersects a cold helium gas jet created by supersonic expansion. Using parallel electric and magnetic fields, both final-state electrons and the recoiling ion are projected onto respective position- and time-sensitive detectors in opposite directions. From the positions of the hits on the detector and their times of flight (TOF), the momentum vectors of the final-state particles are determined. A large part of the entire 4π solid angle is covered, essentially 100% for the detection of the ion and about 80% for the electrons. The latter miss the detector for energies higher than 15 eV transversal to the spectrometer axis and for particular TOF where they arrive close to the spectrometer axis and hit a bore hole in the electron detector, which is required for dumping the projectile beam. For the present measurements, experimental data were obtained from double coincidence events between one of the two outgoing electrons ($\vec{k}_1$) and the recoil ion. The momentum vector of the second electron ($\vec{k}_2$) is obtained using momentum conservation as discussed in [27]. Since all experimental data are measured simultaneously, they are cross normalized, and can be brought to an absolute scale by normalizing to one absolutely known TDCS value within the recorded phase space. This has been done using the absolute TDCS measurements by Ehrhardt and coworkers [14] for $E_0 =$ 65 eV. Due to the slightly lower impact energy a correction factor reflecting the well-known behavior of the total cross section in this energy region was applied.

III. RESULTS AND DISCUSSIONS

The details of the theoretical approaches have already been extensively discussed in [9,10] for CCC, [11,12] for TDCC, [30,33] for BSR, and [8] for DS3C. All calculations have a helium ground state that is sufficiently accurate for the task at hand. Even the frozen-core treatment, where the ground state contains only the $\{1s,nl\}$ configurations, works well for equal-energy sharing ionization down to low energies [10]. Nevertheless for even higher accuracy a multiconfiguration treatment is helpful [34]. In DS3C a simple Slater-type initial state was used. Including radial correlation yields similar results. Some specifics of the coupling schemes used to extract the partial contributions to the TDCS will be discussed below.

The TDCS as 3D emission patterns are presented in Fig. 2 for the experiment (left column) and the CCC calculations (right column) at different scattering angles θ_1. The projectile ($\vec{k}_0$) enters from the bottom and is scattered ($\vec{k}_1$) to the left (hence the minus sign in the notation for θ_1). These two vectors, whose intersection corresponds to the collision point, define the scattering plane as indicated by the solid frame in Fig. 2(c). The TDCS for a particular direction is proportional to the distance from the origin of the plot (also corresponding to the collision point) to the point on the surface that is intersected by the second electron's emission direction.

The measured cross sections shown in the 3D representation are generally governed by the well-known binary and recoil lobes [3,4]: The binary lobe points roughly in the direction of the momentum transfer $\vec{q} = \vec{k}_0 - \vec{k}_1$. Classically this corresponds to electrons emitted after a single binary collision with the projectile. The recoil lobe can be attributed to a binary collision followed by backscattering in the ionic potential, thus resulting in emission roughly along the direction of $-\vec{q}$. The most surprising feature observed in the experiment is the splitting of the binary lobe into two parts. Their relative intensities are strongly dependent on the scattering angle θ_1. It can be seen that the contribution of the binary-B peak is stronger than the binary-A peak for $\theta_1 = -35^\circ$ [Figs. 2(a) and 2(b)], and vice versa for $\theta_1 = -45^\circ$ and -50°, as seen in Figs. 2(e)–2(h). Their relative contributions are about equal for $\theta_1 = -40^\circ$, as seen in Figs. 2(c) and 2(d). This causes a double-peak structure with a dip roughly in the direction of the momentum transfer $\vec{q}$. Given the characteristic momentum

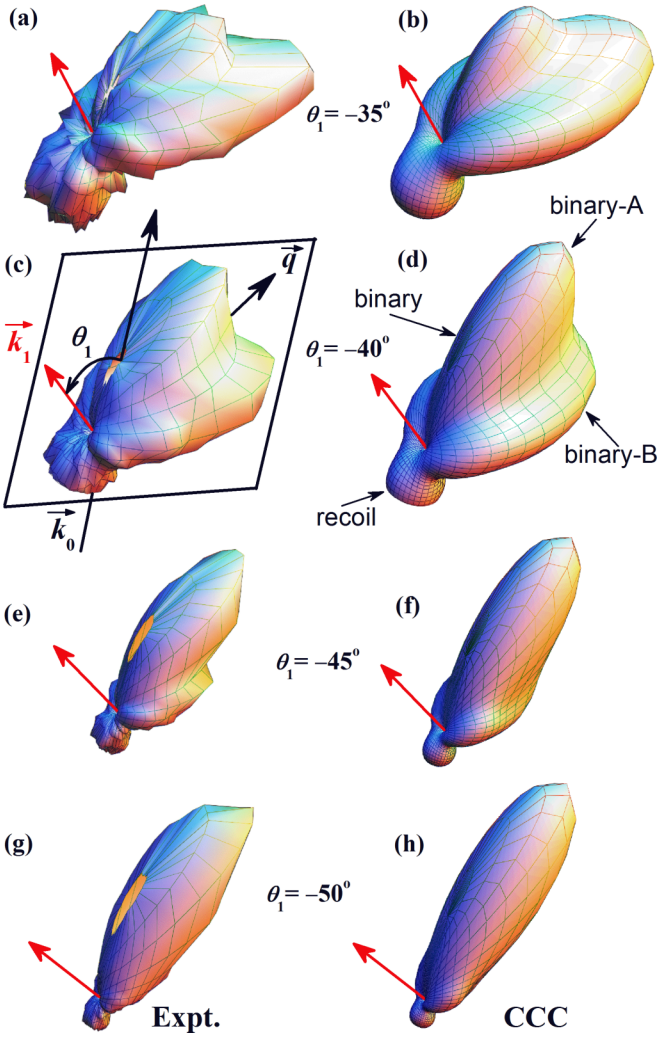

FIG. 2. (Color online) Three-dimensional representation of the TDCS for $(e,2e)$ on He at equal energy sharing ($E_1 = E_2 = 23$ eV) as a function of the emission angle θ_2 of one electron with the other electron's detection angle θ_1 being fixed to (a) and (b) $\theta_1 = -35^\circ$; (c) and (d) $\theta_1 = -40^\circ$; (e) and (f) $\theta_1 = -45^\circ$; (g) and (h) $\theta_1 = -50^\circ$. Left column, experiment; right column, CCC calculation.

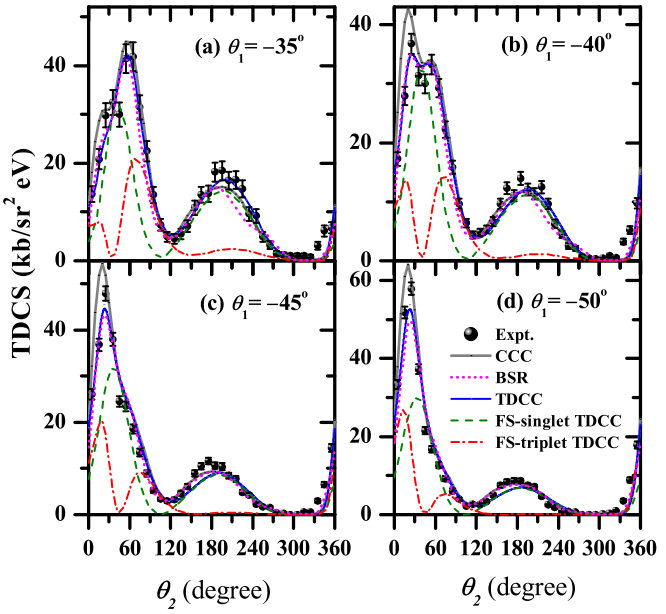

FIG. 3. (Color online) Experimental data compared with CCC, BSR, and TDCC predictions for the TDCS in the scattering plane ($E_1 = E_2 = 23$ eV) as a function of one-electron emission angle (θ_2) with the other electron emission angle θ_1 fixed to -35° (a), -40° (b), -45° (c), and -50° (d). Also shown are the TDCC results for the contributions from the final-state (FS) singlet and triplet spin channels constructed from coupling the spins of the two outgoing electrons. See text for details.

profile of the $1s^2$ ground state of helium, such a minimum is unexpected for this case [35]. Regarding comparison between experiment and theory, all observed features in the 3D image are very well reproduced by theory.

For a more quantitative investigation of the observed structures in the TDCS, cuts through the 3D images of the TDCS are exhibited in Fig. 3. The cross sections in the scattering plane [sketched in Fig. 1 and indicated by the solid frame in Fig. 2(c)] are presented as a function of the emission angle θ_2 with the other electron's detection angle being fixed between -35° and -50°. Also included in Fig. 3 are the theoretical predictions from the CCC, BSR, and TDCC methods. Excellent agreement is obtained between experiment and all theories.

In order to push the analysis further, it is now necessary to discuss in some detail how the TDCS is actually obtained in the various methods. In the TDCC approach, the spin of the incident projectile is coupled to that of the ejected electron to form either a singlet or triplet combined spin of this two-electron subsystem. The interaction between these two electrons is treated exactly. The remaining target electron is treated like a spectator and its spin is not considered at all, although the interaction of the target electrons with the outgoing electrons is included via direct and local exchange potentials. In other words, the active target electron is treated like the valence electron of an alkali-metal atom. Due to the fact that the total spin of the three-electron system is $S_{\rm tot} = 1/2$ (in the nonrelativistic approximation), it is *not appropriate* to associate the contribution to the singlet and triplet amplitudes with "direct" and "exchange" processes, as would be done in collisions with an actual (quasi-)one-electron target. Moreover, in general it is not possible to separate out the direct and exchange contributions within the TDCC approach. In our model, the TDCS is the sum of the singlet and triplet contributions. The triplet cross section vanishes for $\theta_1 = \theta_2$ (see in Fig. 3), as is required by the Pauli principle. This forced zero of the TDCS is then also reflected in the dip structure as found experimentally for $\theta_1 = -40^\circ$, or in shoulders in the binary peak as found for $\theta_1 = -35^\circ$, -45°, and -50°.

A *different* way of splitting up the contributions to the TDCS is employed in the pseudostate close-coupling approach, which is the basis of both the CCC and BSR ways to account for coupling to the ionization continuum. In these models, a two-step process is used. First, one calculates the excitation of discrete (boundlike) pseudostates of the helium target, and in a second step excitation of the states that lie above the physical ionization threshold is reinterpreted as ionization. While the details vary greatly in the two approaches, the basic idea is the

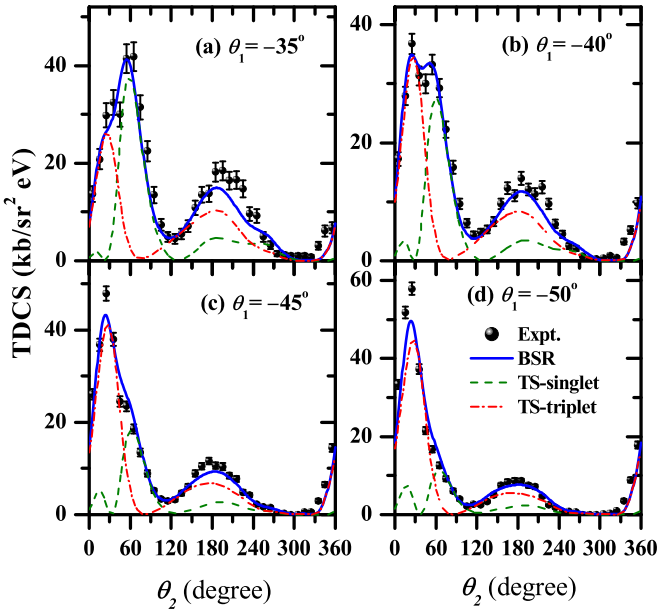

FIG. 4. (Color online) Same as Fig. 3, except that the BSR theory is used to compare with the experimental data. Also shown are the contributions from excitation of the target-state (TS) singlet and triplet. See text for details.

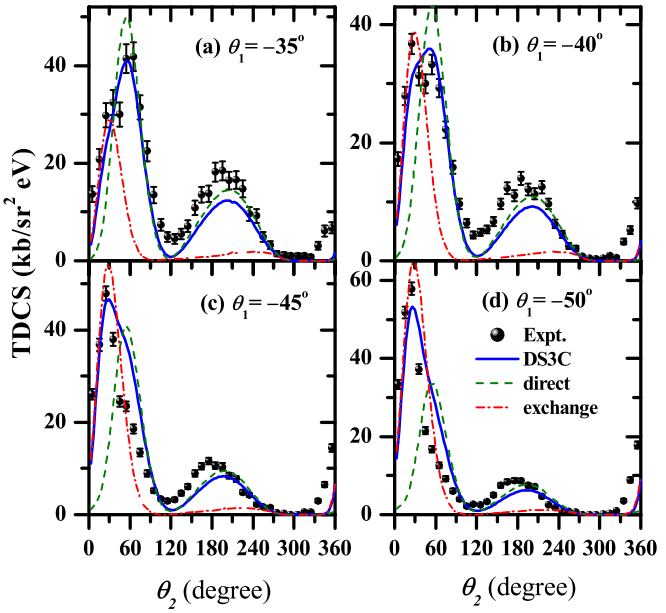

FIG. 5. (Color online) Same as Fig. 3, except that the DS3C theory (solid line) is used to compare with the experimental data. Also shown are the separate direct and exchange contributions. See text for details.

same. Most importantly, these formulations conserve the total spin $S_{\rm tot}$ of the three-electron system. Hence, with the initial bound state being $(1s^2)^1S$, they only allow for $S_{\rm tot} = 1/2$ in the present nonrelativistic approximation. Furthermore, the triplet states of the target can *only* be excited by exchange, while the singlet states could be excited by both direct and exchange processes. In other words, the excitation of the triplet states measures the exchange contribution individually, while the excitation of the singlet states contains the direct process, the exchange process, and their interference.

Looking at the BSR results from the two sets of target states in Fig. 4, we see that the exchange contribution to the binary peak grows when the detection angle θ_1 grows in magnitude. Except for $\theta_1 = -35^\circ$, the binary peak seen at $\theta_2 = 30^\circ$ almost entirely comes from excitation of the triplet states. In other words, there is a propensity that the electron detected at $\theta_2 = 30^\circ$ is actually the original projectile, rather than the electron that is detected at $\theta_1 = -50^\circ$. We also see that the double-peak structure in the TDCS at $\theta_1 = -40^\circ$ is basically caused by the rapid growth of the exchange contribution and the simultaneous decrease of the remainder. We emphasize again that this remainder in the BSR and CCC formalism is not separable into direct and exchange contributions.

An analytical theory can often give detailed insight into the mechanisms of the process studied [36]. In Fig. 5, the experimental TDCS in the scattering plane are compared with predictions from the DS3C model. DS3C also produces good agreement with experiment, except for $\theta_1 = -40^\circ$ where the double-peak structure is indicated but with an apparently different (from experiment and the other theories) weight of the underlying peaks. Furthermore, the binary peaks display a shoulder toward larger angles for $\theta_1 = -45^\circ$ and -50°.

In DS3C the two bound electrons participate in scattering, however, only the roles of the projectile and the continuum electrons are exchanged, giving rise to a direct and exchange amplitude. Note that the TDCS in the DS3C model is not the sum of the direct and exchange contributions, due to interference terms that also enter the formula. In the binary region of the TDCS, for all θ_1 cases presented in Fig. 5, the exchange contribution gives rise to a peak at $\theta_2 = 30^\circ$ while the direct scattering process is responsible for a peak at $\theta_2 \approx 60^\circ$. The relative intensities between these two contributions strongly depend on the fixed electron angle of θ_1. Qualitatively, the results are similar to those obtained in the BSR approach: With increasing magnitude of θ_1, the binary peak moves to smaller values of θ_2, and the exchange contribution to this peak grows. This, once again, supports the propensity of assigning the electron detected at the smaller (absolute) angle is the projectile.

IV. CONCLUSIONS

In summary, we have reported experimental and theoretical results for electron-impact ionization of helium at $E_0 = 70.6$ eV, in which the TDCS for equal energy sharing of the two outgoing electrons ($E_1 = E_2 = 23$ eV) is presented for several scattering angles θ_1. Instead of the general binary and recoil features in the TDCS, we observed a double-peak structure in the binary lobe. The experimental data are best reproduced by the nonperturbative CCC, BSR, and TDCC theories. Based on the spin-coupling scheme used in CCC and BSR, the double-peak structure can be interpreted as a growing propensity for the electron being detected at the smaller angle (relative to the forward direction) to correspond to the original projectile. We hope that the results obtained in this work will help to interpret the electron-impact ionization process also in more complex systems.

ACKNOWLEDGMENTS

This work was supported, in part, by the United States National Science Foundation, the Australian Research Council, the National Computer Infrastructure, and the Pawsey Supercomputer Centre. The Los Alamos National Laboratory is operated by Los Alamos National Security, LLC for the National Nuclear Security Administration of the U.S. Department of Energy under Contract No. DE-AC5206NA25396. The authors are grateful to B. Najjari for valuable discussions. J.B. is supported by the German Research Foundation (DFG) Grants No. SFB 762.

[1] B. Boudaïffa, P. Cloutier, D. Hunting, M. Huels, and L. Sanche, Science **287**, 1658 (2000).
[2] B. C. Garrett, D. A. Dixon, D. M. Camaioni, D. M. Chipman, M. A. Johnson, C. D. Jonah, G. A. Kimmel, J. H. Miller, T. N. Rescigno, P. J. Rossky, S. S. Xantheas, S. D. Colson, A. H. Laufer, D. Ray, P. F. Barbara, D. M. Bartels, K. H. Becker, K. H. Bowen, S. E. Bradforth, I. Carmichael, J. V. Coe, L. R. Corrales, J. P. Cowin, M. Dupuis, K. B. Eisenthal, J. A. Franz, M. S. Gutowski, K. D. Jordan, B. D. Kay, J. A. LaVerne, S. V. Lymar, T. E. Madey, C. W. McCurdy, D. Meisel, S. Mukamel, A. R. Nilsson, T. M. Orlando, N. G. Petrik, S. M. Pimblott, J. R. Rustad, G. K. Schenter, S. J. Singer, A. Tokmakoff, L.-S. Wang, and T. S. Zwier, Chem. Rev. **105**, 355 (2005).
[3] H. Ehrhardt, K. Jung, G. Knoth, and P. Schlemmer, Z. Phys. D **1**, 3 (1986).
[4] A. Lahmam-Bennani, J. Phys. B **24**, 2401 (1991).
[5] M. Brauner, J. S. Briggs, and H. Klar, J. Phys. B **22**, 2265 (1989).
[6] B. Brauner, J. S. Briggs, H. Klar, J. T. Broad, T. Rosel, K. Jung, and H. Ehrhardt, J. Phys. B **24**, 657 (1991).
[7] J. Berakdar and J. S. Briggs, J. Phys. B **29**, 2289 (1996).
[8] J. Berakdar and J. S. Briggs, Phys. Rev. Lett. **72**, 3799 (1994).
[9] I. Bray and D. V. Fursa, Phys. Rev. A **54**, 2991 (1996).
[10] A. T. Stelbovics, I. Bray, D. V. Fursa, and K. Bartschat, Phys. Rev. A **71**, 052716 (2005).
[11] J. Colgan, M. S. Pindzola, G. Childers, and M. A. Khakoo, Phys. Rev. A **73**, 042710 (2006).
[12] J. Colgan, M. Foster, M. S. Pindzola, I. Bray, A. T. Stelbovics, and D. V. Fursa, J. Phys. B **42**, 145002 (2009).
[13] T. N. Resigno, M. Baertschy, W. A. Isaacs, and C. W. McCurdy, Science **286**, 2474 (1999).
[14] I. Bray, D. V. Fursa, J. Röder, and H. Ehrhardt, J. Phys. B **30**, L101 (1997).
[15] X. Ren, A. Dorn, and J. Ullrich, Phys. Rev. Lett. **101**, 093201 (2008).
[16] A. Naja, E. M. S. Casagrande, A. Lahmam-Bennani, M. Stevenson, B. Lohmann, C. D. Cappello, K. Bartschat, A. Kheifets, I. Bray, and D. V. Fursa, J. Phys. B **41**, 085205 (2008).
[17] M. A. Stevenson, L. R. Hargreaves, B. Lohmann, I. Bray, D. V. Fursa, K. Bartschat, and A. Kheifets, Phys. Rev. A **79**, 012709 (2009).
[18] X. Ren, A. Senftleben, T. Pflüger, A. Dorn, K. Bartschat, and J. Ullrich, J. Phys. B **43**, 035202 (2010).
[19] O. Zatsarinny and K. Bartschat, Phys. Rev. Lett. **107**, 023203 (2011).
[20] X. Ren, I. Bray, D. V. Fursa, J. Colgan, M. S. Pindzola, T. Pflüger, A. Senftleben, S. Xu, A. Dorn, and J. Ullrich, Phys. Rev. A **83**, 052711 (2011).
[21] A. J. Murray and F. H. Read, J. Phys. B **26**, L359 (1993).
[22] X. Ren, A. Senftleben, T. Pflüger, A. Dorn, K. Bartschat, and J. Ullrich, Phys. Rev. A **83**, 052714 (2011).
[23] S. Amami, M. Ulu, Z. N. Ozer, M. Yavuz, S. Kazgoz, M. Dogan, O. Zatsarinny, K. Bartschat, and D. Madison, Phys. Rev. A **90**, 012704 (2014).
[24] X. Ren, S. Amami, O. Zatsarinny, T. Pflüger, M. Weyland, W. Y. Baek, H. Rabus, K. Bartschat, D. Madison, and A. Dorn, Phys. Rev. A **91**, 032707 (2015).
[25] E. Ali, X. Ren, A. Dorn, C. Ning, and D. Madison, J. Phys. B **48**, 115201 (2015).
[26] O. Al-Hagan, C. Kaiser, A. J. Murray, and D. Madison, Nat. Phys. **5**, 59 (2009).
[27] X. Ren, A. Senftleben, T. Pflüger, A. Dorn, J. Colgan, M. S. Pindzola, O. Al-Hagan, D. H. Madison, I. Bray, D. V. Fursa, and J. Ullrich, Phys. Rev. A **82**, 032712 (2010).
[28] K. L. Nixon, A. J. Murray, H. Chaluvadi, S. Amami, D. H. Madison, and C. Ning, J. Chem. Phys. **136**, 094302 (2012).
[29] X. Ren, T. Pflüger, S. Xu, J. Colgan, M. S. Pindzola, A. Senftleben, J. Ullrich, and A. Dorn, Phys. Rev. Lett. **109**, 123202 (2012).
[30] O. Zatsarinny and K. Bartschat, Phys. Rev. A **85**, 062709 (2012).
[31] D. H. Phillips and M. R. C. McDowell, J. Phys. B **6**, L165 (1973).
[32] J. Ullrich, R. Moshammer, A. Dorn, R. Dörner, L. Schmidt, and H. Schmidt-Böcking, Rep. Prog. Phys. **66**, 1463 (2003).
[33] O. Zatsarinny and K. Bartschat, J. Phys. B **46**, 112001 (2013).
[34] I. Bray and D. V. Fursa, J. Phys. B **44**, 061001 (2011).
[35] I. E. McCarthy and E. Weigold, Rep. Prog. Phys. **54**, 789 (1991).
[36] J. Berakdar and J. S. Briggs, J. Phys. B **27**, 4271 (1994).